




# Isolation and Identification of a *Bacillus* sp. from Freshwater Sediment Displaying Potent Activity Against Bacteria and Phytopathogen Fungi

Miladis I. Camacho<sup>1</sup> · Janet M. García<sup>2</sup> · Dianelis Roget<sup>3</sup> · Armando Ferrer<sup>4</sup> · Anneleen D. Wieme<sup>5</sup> · Peter Vandamme<sup>5,6</sup> · Suyén Rodríguez<sup>7</sup> · Gabriel Llauradó<sup>1</sup>  · Yaneisy Lescaylle<sup>1</sup> · Leonor Peña<sup>1</sup> · Javier Bonne<sup>6</sup> · Thais-Len Meriño<sup>8</sup>

Received: 21 March 2022 / Accepted: 14 October 2022 / Published online: 9 November 2022  
© The Author(s), under exclusive licence to Springer Science+Business Media, LLC, part of Springer Nature 2022

## Abstract

A bacterium strain isolated from freshwater sediment of San Pablo river of Santiago de Cuba, Cuba was identified as a *Bacillus* sp. by Matrix-Assisted Laser Desorption/Ionization Time Of Flight Mass Spectrometry. A 16S rRNA gene analysis showed that the isolate A3 belongs to the operational group *Bacillus amyloliquefaciens*, while the phylogenetic analysis of the *gyrA* gene sequence grouped it within *B. amyloliquefaciens* subsp. *plantarum* cluster, referred now as *Bacillus velezensis*. In vitro antibacterial studies demonstrated the capacity of the isolate A3 to produce bioactive metabolites against *Bacillus subtilis* ATCC 11,778, *Bacillus cereus* ATCC 6633, and *Staphylococcus aureus* ATCC 25,923 by cross-streak, overlay, and microdilution methods. The strain also showed a high potential against the multidrug-resistant *Staphylococcus aureus* ATCC 700,699, ATCC 29,213, and ATCC 6538. At pH 8 and 96 h in the medium 2 of A3 culture conditions, the produced metabolites with antibacterial potential were enhanced. Some alterations in the morphology of the phytopathogens *Aspergillus niger* ATCC 9642, *Alternaria alternata* CECT 2662, and *Fusarium solani* CCEBI 3094 were induced by the cell-free supernatant of *B. velezensis* A3. A preliminary study of the nature of the bioactive compounds produced by the strain A3 showed the presence of both lipids and peptides in the culture. Those results highlight *B. velezensis* A3 as a promissory bacterium capable to produce bioactive metabolites with antibacterial and antifungal properties against pathogens.

## Introduction

The appearance of multidrug-resistant bacteria is one of the problems that affect the worldwide health, with a great incidence of methicillin-resistant *Staphylococcus aureus* (MRSA), vancomycin-resistant enterococcus, and

beta-lactamase producing Gram-negative bacteria [1]. Furthermore, the use and overuse of these therapeutic compounds in the agriculture and veterinary have generated globally various problems [2]. Fungi of the genera *Aspergillus*, *Alternaria*, and *Fusarium* represent a threat to both agricultural production and human health. Several public

✉ Gabriel Llauradó  
gabriel@uo.edu.cu; gabocuba@gmail.com

<sup>1</sup> Centro de Estudios de Biotecnología Industrial (CEBI), Faculty of Natural and Exact Sciences, University of Oriente, Patricio Lumumba, 90500 Santiago de Cuba, Cuba

<sup>2</sup> Cayo Naranjo Dolphinarium, UEB Marina Gaviota Oriente, Naranjo Bay, Km 58 Guardalavaca Highway, Rafael Freyre, Holguin, Cuba

<sup>3</sup> Cuban Institute for Research On Sugar Cane Derivatives, Via Blanca 804, San Miguel del Padrón, La Habana, Cuba

<sup>4</sup> Chemistry Department, Faculty of Exact and Natural Sciences, Universidad de Oriente, Patricio Lumumba, 90500 Santiago de Cuba, Cuba

<sup>5</sup> BCCM/LMG Bacteria Collection, Laboratory of Microbiology, Faculty of Sciences, Ghent University, K.L. Ledeganckstraat 35, 9000 Ghent, Belgium

<sup>6</sup> Laboratory of Microbiology, Faculty of Sciences, Ghent University, K.L. Ledeganckstraat 35, 9000 Ghent, Belgium

<sup>7</sup> Laboratory of Antibodies and Experimental Biomodels, Prolongation of 23th Street and Caney Highway, Vista Alegre, Santiago de Cuba, Cuba

<sup>8</sup> Laboratory of Hygiene, Epidemiology and Microbiology, J Street, Between 1st and 2nd, Sueño Neighborhood, Santiago de Cuba, Cuba

health organizations have cataloged this resistance as a “crisis” or “nightmare scenario” that could have “catastrophic consequences” [3]. Therefore, to find new bioactive metabolites (BMs) with novel action mechanisms to overcome this current problem is an urgent necessity.

Several *Bacillus* spp. have been identified as good antibiotic-producers. They produce lipopeptides and non-ribosomal peptides with different structures and biological activities [4]. In this sense, *Bacillus amyloliquefaciens* group species commonly produce compounds that promote plant growth and that are effective against pathogenic microorganisms [5, 6].

MALDI-TOF MS (Matrix-Assisted Laser Desorption/Ionization in Time of Flight Mass Spectrometry) has emerged as a powerful high-throughput tool in the taxonomic identification and diagnosis of bacteria [7]. Various *Bacillus* spp. and *Bacillus*-like strains have been accurately identified using this phenotypic technique [8, 9]. However, one of its challenges in the bacterial identification might arise from close-relatedness species [10].

Traditionally, the phylogeny and taxonomy of members of genus *Bacillus* have been delimited through the sequencing of 16S rRNA gene. But, the limited taxonomic resolution of this gene among closely related bacteria prevents accurate species level identification of several clusters of closely related *Bacillus* species [11]. Protein-coding genes exhibit much higher genetic variation and can be used for classification and identification of closely related taxa of this genus [12].

In this study, the strain A3 was isolated from the freshwater sediment of San Pablo river, Santiago de Cuba city, Cuba. The bacterium was taxonomically identified using MALDI-TOF MS, and the analysis of the genes 16S rRNA and *gyrA*. Its antibacterial and antifungal activity was screened. Alterations of the morphology of the phytopathogen in interaction with the strain A3 were also examined via microscopy studies. Optimal conditions for a higher metabolite production were determined. Finally, a preliminary study to know the possible nature of the BMs produced by strain A3 was performed as well.

## Materials and Methods

### Sample Collection and Isolation

Strain A3 was isolated from sediment sample of the San Pablo river, La Risueña community, Santiago de Cuba, Cuba, positioned at  $-75^{\circ}49'21.9''$  (N) and  $20^{\circ}3'36.7''$  (W). The sample was aseptically taken in nylon bags at a depth of 27.0 cm and stored at 4 °C. One gram of fresh sediment was added into 9 ml sterilized distilled water and vigorously shaken on a vortex mixer. Then, 1 ml of sediment

suspension was cultivated at room temperature in a 250 ml Erlenmeyer flask with 100 ml of nutrient broth (BioCen) for 24 h, while shaking at 120 rpm. Multiple serial dilutions ( $10^{-1}$ – $10^{-8}$ ) were prepared and placed in a thermostatic bath at 55 °C for 15 min, and 100  $\mu$ l of the culture was spread onto starch-casein agar (composition (g/l): starch, 10; casein, 0.3; KNO<sub>3</sub>, 2.0; K<sub>2</sub>HPO<sub>4</sub>, 2.0; MgSO<sub>4</sub>·7H<sub>2</sub>O, 0.05; CaCO<sub>3</sub>, 0.02; FeSO<sub>4</sub>·7H<sub>2</sub>O, 0.01; pH 7.0). The plates were incubated at 30 °C for 7 days. Bacterial isolate was selected to sub-culture on tryptone soy agar (Oxoid) and confirmed by the Gram's stain.

### Preliminary Screening of Isolate A3 for Antibacterial and Antifungal Activities

#### Antibacterial Activity

The in vitro antibacterial screening was performed by disk-diffusion method [13] against the reference Gram-positive bacteria *Bacillus subtilis* ATCC 11778, *Bacillus cereus* ATCC 6633, and *Staphylococcus aureus* ATCC 25923. The isolate A3 was cultivated in tryptone soya broth (TSB; BioCen) at room temperature for 96 h. The culture was centrifuged (15 min at 8000 rpm) and filtered sterilized through bacteriological filter (0.22  $\mu$ m) into sterile screw-capped glass vials. Sterilized paper disks of 6 mm of diameter were impregnated with 20  $\mu$ l of the free-cell culture, and placed them into Müeller-Hinton agar (MHA) plates. Prior, the plates were spread with 100  $\mu$ l of a culture adjusted to 0.5 McFarland standard ( $1-5 \times 10^8$  CFU/ml) of the test bacteria. A clear zone around the colony evidenced a positive antibacterial activity and was expressed as the diameter of zone of inhibition in mm.

A further antibacterial screening was tested only against the multidrug-resistant strains *S. aureus* ATCC 700699 and *S. aureus* ATCC 29213 using the overlay method, according the procedures of the LMG bacteria culture collection, University of Ghent, Belgium. The bacterium A3 was grown on tryptone soya agar (TSA; Oxoid) at 37 °C for 24–48 h and tested against the pathogen bacteria. A dissolution of TTC (2,3,5-triphenyltetrazolium chloride) redox indicator was added to the culture with a final concentration of 0.02% (w/v) and used as revelator to visualize a positive anti-staphylococci activity.

#### Antifungal Activity

The antifungal activity was performed through the determination of the percentage of inhibition of the radial growth (PIRG) of *Alternaria alternata* CECT 2662, *Aspergillus niger* ATCC 9642, and *Fusarium solani* CCEBI 3094 by agar well-diffusion method [14]. The phytopathogen fungi were cultivated on petri dishes with malta agar medium

(MA) for 5–7 days at 30 °C. One plug of mycelium (6 mm of diameter) was placed at the center of MA petri dishes. Twenty microliters of the A3 supernatant was transferred into the wells of 6 mm diameter made with a cork borer at a distance of 30 mm of the center. Then, the plates were kept for one hour at room temperature (25–27 °C) for a well diffusion of the cell-free culture through the agar, and incubated at 30 °C for 7 days. The PIRG was measured according the following expression:

$$\text{PIRG (\%)} = R1 - R2/R1 \times 100$$

R1 is the average value of the colony radius (mm), and R2 is the average value of the inhibited colony radius (mm).

### Secondary Screening by Broth Microdilution Method

The extracellular metabolites released by A3 in TSB medium were extracted with chloroform and n-butanol solvents, and tested only against *S. aureus* ATCC 6538 by broth microdilution method. The organic phases were collected by using a separating funnel and evaporated to dryness employing a rotatory evaporator with a slight rotation at 45 °C. The extracts were dissolved at a concentration 20 mg/ml in dimethyl sulfoxide and tested in a 96-well microtiter plate according to the protocols from the Laboratory of Microbiology, Parasitology and Hygiene (University of Antwerp, Belgium) [15].

### Selection of Suitable Conditions for Maximum Production of BMs by Isolate A3

#### Culture Media

Four culture media were tested to improve the production of BMs by the bacterial isolate: medium 1 [composition (g/l): yeast extract, 3; soluble starch 5;  $\text{NH}_4(\text{SO}_4)_2$ , 2], medium 2-ISP2 [composition (g/l): malt extract, 10; yeast extract, 4; dextrose, 4], medium 3 [composition (g/l): soluble starch, 10; yeast extract, 4; peptone, 2;  $\text{CaCO}_3$ , 10;  $\text{Fe}(\text{SO}_4)_3$ , 8], and medium 4 [composition (g/l): dextrose, 32.5; soy trypticase broth, 9]. All culture media were adjusted at pH 7. Ten milliliters of each media were inoculated with 10% (v/v) of a culture of A3 in TSB kept in shaking at 200 rpm during 24 h at 37 °C. Supernatants were obtained as described above and subjected to disk-diffusion assay against *B. cereus* ATCC 6633.

#### Incubation Time

The suitable incubation time was determined by adding a seed inoculum of A3 at a concentration of 10% (v/v) in 10 ml of medium 2. Samples were taken at 48, 96, and 168 h,

and used to determine the antibacterial potential against *B. cereus* ATCC 6633 as described before.

#### pH

Optimum pH for the maximum production of BMs by A3 was determined by seeding an inoculum of 10% (v/v) in 10 ml of medium 2 adjusted to pH values of 6, 7, 8, and 9 using 0.1 N NaOH and 0.1 M HCl before sterilization. The incubation was done at 37 °C at 200 rpm for 96 h. Antibacterial activity of supernatants was similar to the early performed.

#### Inoculum Size

Erlenmeyer flasks with 10 ml of ISP2 medium, adjusted at pH 8, were seeded with inoculums of the isolate A3 at concentrations of 5, 10, and 20% (v/v) to test the maximum production of BMs. Incubation and antibacterial activity were carried out as above mentioned.

### Preliminary Chemical Screening of the BMs Produced by *B. velezensis* A3

#### Thin-Layer Chromatography (TLC)

A thin-layer chromatography using silica gel plates RP-18F254S (Merck), 5 × 10 cm, 0.25 mm thick was performed. The culture was loaded on the plates with the help of capillary tube. Single chromatographies to determine the presence of peptides/amino acids, lipids, and reducer sugars in the culture of the strain A3 were performed. A mobile phase consisting of n-butanol–acetic acid–water (4:4:2) was prepared for determining peptides compounds. The TLC plate was sprayed uniformly with ninhydrin solution (0.2% in distilled water) and placed to dry at room temperature. The presence of blue violet spots indicated the presence of both peptides/amino acids compounds when the TLC plates were observed with a transilluminator.

A chloroform–toluene (85:15) mixture was used to detect the presence of lipids. The plates were revealed with 10% (v/v) phosphomolybdic acid in absolute ethanol. The stained sheets were heated at 110 °C for 10–15 min. Blue spots indicated a positive result for this compound.

Reducer sugars were detected by using methanol–n-butanol–phosphate buffer pH 7 [5:4:1 (v/v)]. MTT [3-(4,5-dimethylthiazol-2-yl)-2,5-diphenyltetrazolium bromide] was used as revelator. Retardation factor (Rf) values of the spots were calculated.

## UV–Vis Spectrophotometry

The UV–vis spectra of the BMs produced by A3 were obtained and recorded on a Spectrophotometer Ray Leigh UV-2601 (China) at wavelengths from 200 to 800 nm. Sample was prepared taken into account the optimal conditions for the maximum production of BMs by A3.

## Taxonomic Studies

### MALDI-TOF MS

Strain A3 was identified by MALDI-TOF MS. Isolate was subcultured thrice on TSA, and MALDI-TOF MS was performed using the third generation of pure cultures by means of a 4800 Plus MALDI-TOF/TOF™ Analyzer (AB SCIEX, Framingham, MA, USA), as was previously described by Wieme et al. [16]. The spectrum was visualized with *mMass* program version 5.5.0 [17].

### 16S rRNA Gene Sequencing

In order to corroborate the MALDI-TOF taxonomic identification, further 16S rRNA gene sequencing was performed as was described by [18]. For sequencing, the primers \*Gamma (5'-CTC CTA CGG GAG GCA GT-3') and BKL1 (3'-GTA TTA CCG CGG CTG CTG GCA-5') were used. The resulting partial sequence of strain A3 was used to compare with those reference strains from EZBioCloud database [19]. The multiple alignments were done against the SILVA SSU reference database using SINA (v1.2.11) (<https://www.arb-silva.de/aligner/>) [20]. The neighbor-joining [21], maximum-likelihood [22], and maximum-parsimony [23] methods were used for phylogenetic tree reconstruction using the software MEGA version 7.0.26 [24]. Evolutionary distances were calculated using Kimura two-parameter model [25]. A discrete Gamma distribution was used to model evolutionary rate differences among sites, and the rate variation model allowed for some sites to be evolutionarily invariable. The confidence values of branches of the phylogenetic trees were determined using bootstrap analysis based on 1000 resamplings. Gaps and ambiguous nucleotides were eliminated from the calculations.

### *gyrA* Gene Sequencing

We also attempted to amplify and sequence the *gyrA* gene (DNA gyrase subunit A) as was described by Chun and Bae [26]. A multiple alignment of the *gyrA* gene sequence of strain A3 against fifty-eight sequences of *Bacillus subtilis* group was carried out using the MUSCLE tool [27] available in the MEGA v.7.0.26 software [24]. The phylogenetic

trees were constructed as previously described. Evolutionary distances were also calculated using Kimura two-parameter model [25] with a gamma-distributed among site rate variation.

## Nucleotide Sequence Accession Number

The 16S rRNA gene and *gyrA* gene sequences were deposited in the GenBank/EMBL/DDDBJ databases with the accession number MG545728 and MG641042, respectively.

## Results

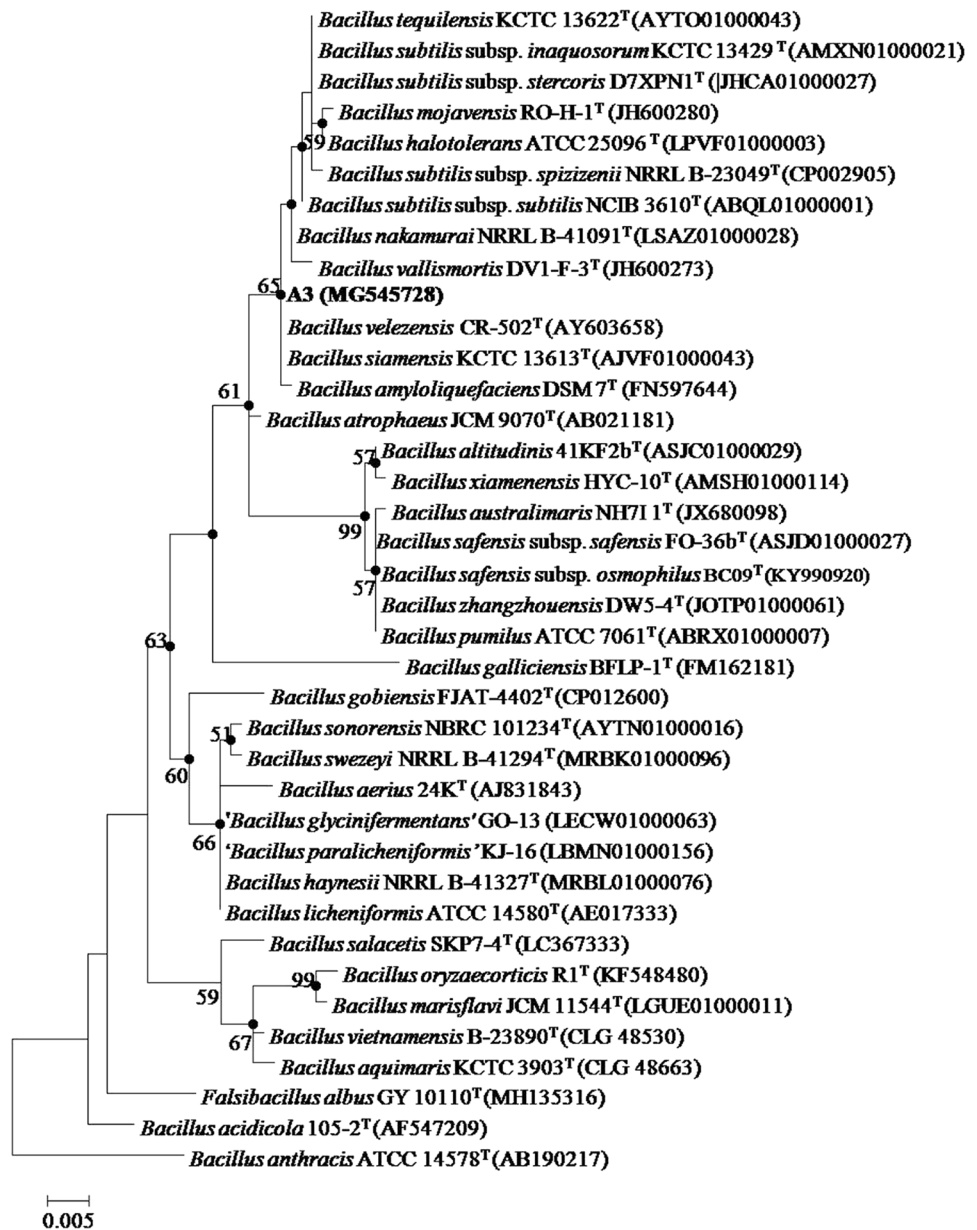
### Isolation and Characterization of Isolate A3

In this study, 106 bacteria were isolated from freshwater sediment of San Pablo river. Preliminary screening was carried out for all strains that inhibited the growth of *B. cereus* ATCC 6633, *B. subtilis* ATCC 11778, and *S. aureus* ATCC 25923. Strain A3 was chosen by having a higher antibacterial and antifungal potential. Microscopical observations evidenced that A3 is a rod-shaped, endospore-forming Gram-positive bacterium with a wrinkled appearance on TSA medium.

### Taxonomic Identification of Isolate A3

The mass spectrum profile of A3 evidenced an incongruent taxonomic identification toward *Bacillus amyloliquefaciens* and *Bacillus methylotrophicus* with scores of 2.5 and 2.3, respectively. The partial 16S rRNA gene sequence (1204 nt) was subsequently compared with sequences in the EzBioCloud database, and the results confirmed that the strain A3 belongs to the genus *Bacillus*. Strain A3 was closely related to *Bacillus velezensis* CR-502<sup>T</sup> (100%), *Bacillus siamensis* KCTC 13613<sup>T</sup> (99.9%), *Bacillus amyloliquefaciens* DMS7<sup>T</sup> (99.7%), *Bacillus subtilis* subsp. *subtilis* (99.7%), *Bacillus nakamurai* NRRL B-41091<sup>T</sup> (99.7%), *Bacillus tequilensis* KCTC 13622<sup>T</sup> (99.6%), *Bacillus subtilis* subsp. *inaquosorum* KCTC 13429<sup>T</sup> (99.6%), *Bacillus atrophaeus* JCM 9070<sup>T</sup> (99.5%), *Bacillus valimortis* DV1-F-3<sup>T</sup> (99.5%), *Bacillus subtilis* subsp. *stercoris* D7XPN1<sup>T</sup> (99.5%), *Bacillus mojavensis* RO-H-1<sup>T</sup> (99.4%), *Bacillus subtilis* subsp. *spizizenii* NRRL B-23049<sup>T</sup> (99.4%), and *Bacillus halotolerans* ATCC 25096<sup>T</sup> (99.4%). Phylogenetic analysis placed the strain A3 into the “Operational group *B. amyloliquefaciens*” (belonging to *Bacillus subtilis* complex) as ML, NJ, and MP treeing algorithms showed (Fig. 1).

**Fig. 1** Maximum likelihood tree based on partial 16S rRNA gene sequence (842 bp) of isolate A3 showing its phylogenetic position within *Bacillus subtilis* complex strains. The evolutionary distances were computed using Kimura two-parameter model. A discrete Gamma distribution was used to model evolutionary rate differences among sites (5 categories (+G, parameter=0.5681)). The rate variation model allowed for some sites to be evolutionarily invariable ([+I], 45.87% sites). Bootstrap percentage values ( $\geq 50$ ), based on 1000 replications, are shown at branch points. *Bacillus anthracis* ATCC 14578<sup>T</sup> was used as an outgroup. Black dots mean those branches that match with Neighbor-Joining and Maximum Parsimony trees. Bar, 0.005 substitutions per nucleotide position

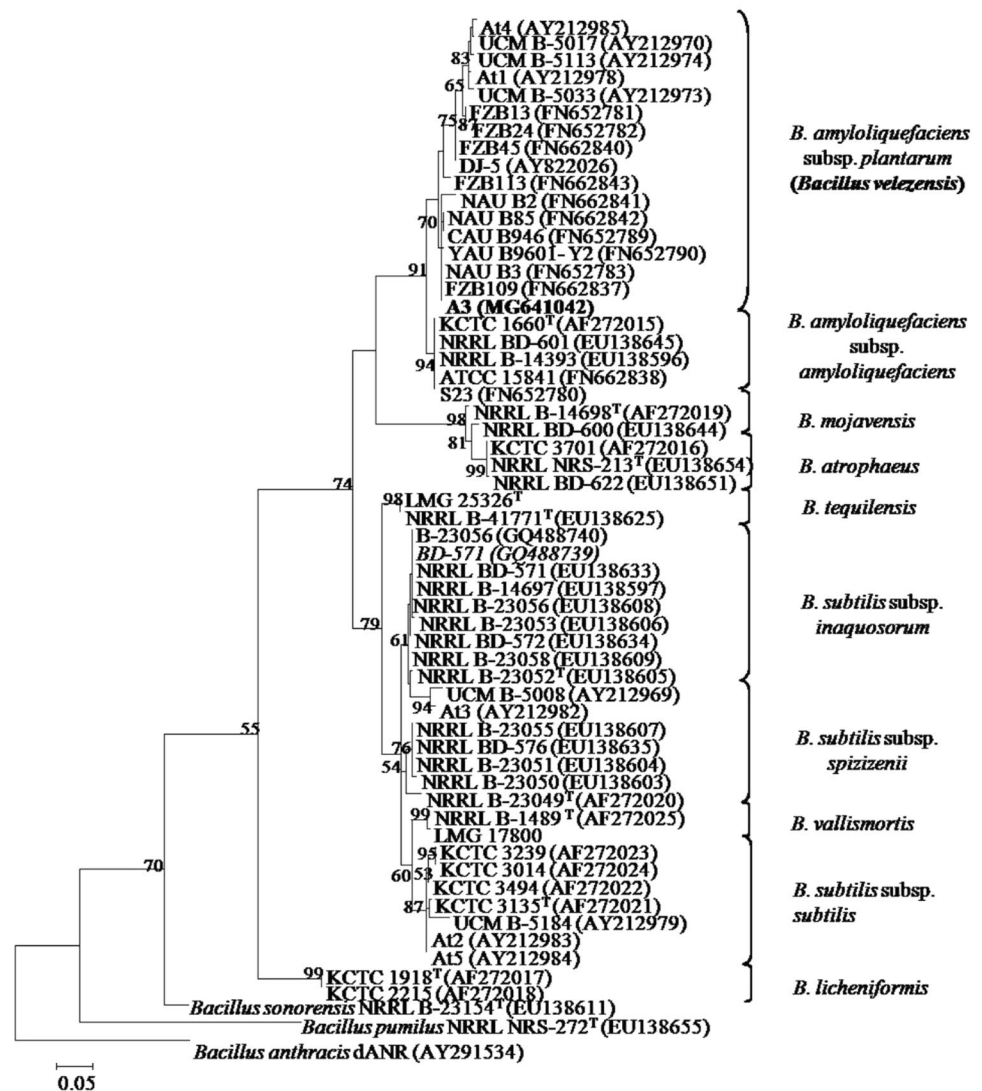


We performed a further *gyrA* (DNA gyrase subunit A) gene sequence analysis to clarify the degree of strain A3's relatedness with its nearest phylogenetic neighbors. The phylogenetic analysis of *gyrA* gene sequence (827 nt) placed the strain A3 within the clade of *B. amyloliquefaciens* subsp. *plantarum* strains (Fig. 2). An additional analysis with thirteen reference strains of *B. velezensis* available on NCBI database (<https://www.ncbi.nlm.nih.gov>) confirmed its classification within this taxon (Supplementary material; Fig. A1).

### Antibacterial Activity of A3

Cell-free supernatant of *B. velezensis* A3 showed a growth inhibition toward *B. cereus* ATCC 6633, *B. subtilis* ATCC 11778, and *S. aureus* ATCC 25923 of  $16.5 \pm 0.7$  mm,  $17.0 \pm 1.4$  mm, and  $11.5 \pm 0.7$  mm, respectively, by disk-diffusion method. The effect of the cell-free supernatant against the pathogenic bacterium ATCC 25923 was noted. Therefore, a further study on the activity of the strain A3 included different multi-resistant *S. aureus* strains. A growth inhibition zone of  $19.0 \pm 0.4$  mm, approximately, was observed when the whole cells of A3 were tested against *S. aureus* ATCC 29213 and *S. aureus* ATCC 700699 by overlay method. The chloroform extract evidenced an  $IC_{50}$  against

**Fig. 2** Maximum likelihood tree based on partial *gyrA* gene sequence (312 bp) of isolate A3 showing its phylogenetic position into the clade of *Bacillus amyloliquefaciens* subsp. *plantarum* (*Bacillus velezensis*). The evolutionary distances were computed using Kimura two-parameter model. A discrete Gamma distribution was used to model evolutionary rate differences among sites [5 categories (+ G, parameter = 0.2678)]. Bootstrap percentages values ( $\geq 50$ ), based on 1000 replications, are shown at branch points. *Bacillus anthracis* dANR was used as an outgroup. Bar, 0.05 substitutions per nucleotide position



*S. aureus* ATCC 6538 of 84.18  $\mu\text{g/ml}$ . The n-butanol extract did not show any antagonist effect against this pathogenic bacterium.

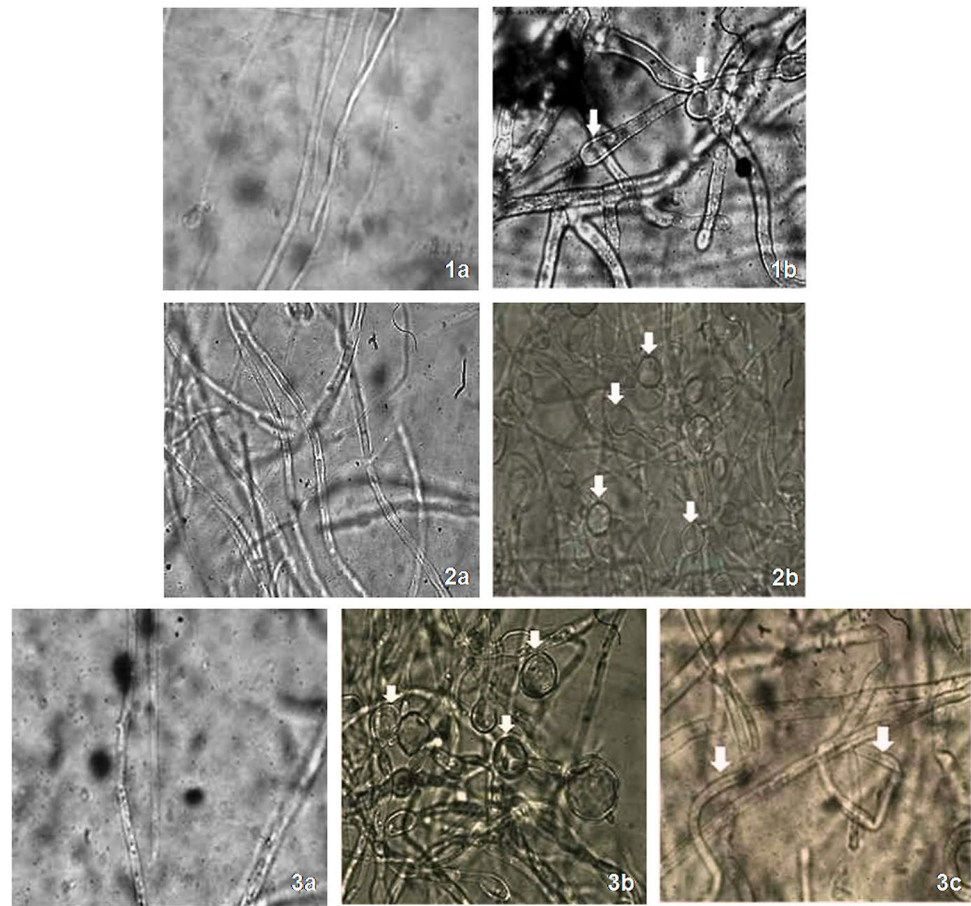
### Antifungal Activity of A3

Supernants of A3 inhibited the radial growth of *A. alternata* CECT 2662, *A. niger* ATCC 9642, and *F. solani* CCEBI 3094 in a 53, 35, and 25%, respectively. Microscopical observations showed alterations in the hyphae of the phytopathogenic fungi related with the hyphae swelling, bulb formation, hyphae twist, zig-zag growth, and abundant vacuolization (Fig. 3).

### Optimization of Culture Media, Incubation Time pH, and Inoculum Size for the Maximum Production of BMs by A3

Antibacterial activity results of strain A3 against *B. cereus* ATCC 6633 by disk-diffusion method according the suitable conditions to produce BMs are shown in Table 1. The recorded results showed that the strain grew in all culture media. However, A3 showed an antibacterial activity when it was cultivated in the media 2 and 4 only. Medium 2 was considered the most suitable for the best production of BMs (Table 1). The maximum BMs production was yielded at the 96 h, supported by the larger hale of inhibition, although an initial antibacterial activity was observed at 48 h (2 days). The study of the pH effect (6, 7, 8, and 9) through multiple range test showed statistically significant differences ( $p=0.0348$ ; 95.0% level of confidence) when A3 was cultivated at pH 6–7 and pH 8–9 for the highest productivity

**Fig. 3** Microphotographies (1000x) showing the alterations produced by BMs of *Bacillus velezensis* A3 in the hyphae of *Fusarium solani* CCEBI 3094 (1), *Alternaria alternata* CECT 2662 (2), and *Aspergillus niger* ATCC 9642 (3). Control (a); hyphae swelling and bulb formation (1b, 2b, and 3b), hyphae twist and zig-zag growth (3c)



of BMs. The inoculum size had not a significant influence in the production of BMs by A3, but the better antibacterial activity was obtained with an inoculum of 20%.

### Preliminary Characterization of the Nature of the BMs Produced by *B. velezensis* A3

The detection of blue violet spots in the chromatography plate indicated the presence of peptide/amino acids compounds (Fig. 4a). Blue spots were also observed when the plates were sprayed with phosphomolibdic acid in ethanol indicating the presence of lipid compounds (Fig. 4b). The presence of reducing sugars was also demonstrated by the apparition of violet spots on a yellow background (Fig. 4c). Additional chemical assays (Supplementary material; Fig. A2a and Fig. A2b) with the Dragendorff reactive and potassium permanganate supported the presence of amino acids (pink precipitate) and compounds with unsaturations (dark brown precipitate), respectively. A low concentration of reducing sugar equivalent to  $2.4 \pm 0.6$  mg/ml was obtained using anthrone method. On the other hand, the TLC results showed spots with Rf values of 0.66 for petroleum extract and, 0.19 and 0.64 for

n-butanol extract in the detection of peptides/amino acid residues. For lipids detection, a diffuse spot at the origin of the application point (Rf = 0) was observed for the n-butanol extract. TLC-reducing sugars evidenced spots with Rf = 0.6 and Rf = 0.43 for n-butanol and petroleum extracts, respectively.

For determine the BMs UV-Vis spectra, a diluted fraction in ISP2 medium (1:3) was scanned by the spectrophotometer previously mentioned. Figure 5 shows the absorption results within the range from 250 to 600 nm, characterized by a wide asymmetric band with overlapped bands around 293 to 480 nm, approximately. The highest intensity occurred at 315 nm. Partially occluded bands (referred as “shoulders”), with a third part of intensity less than the first bands, were observed at 350 and 392 nm.

### Discussion

Screening for new antibiotics from natural sources is becoming increasingly important for the biopharmaceutical industry. Microorganisms represent a promissory source of novel medically, veterinary, and agriculturally

**Table 1** In vitro antibacterial activity of *B. velezensis* A3 against *B. cereus* ATCC 6633 under standardized conditions

Culture conditions		Antibacterial activity (mm)
Culture media	1	–
	2	8.25 ± 0.4 <sup>a</sup>
	3	–
	4	7.0 ± 0.0 <sup>b</sup>
Incubation time (h)	48	7.5 ± 0.5 <sup>a</sup>
	96	16.0 ± 1.4 <sup>b</sup>
	168	8.0 ± 1.4 <sup>c</sup>
pH	6	12.3 ± 1.5 <sup>a</sup>
	7	12.3 ± 2.6 <sup>a</sup>
	8	17.0 ± 3.6 <sup>b</sup>
	9	16.8 ± 1.5 <sup>b</sup>
Inoculum size (%)	1	14.5 ± 2.1 <sup>a</sup>
	5	19.0 ± 1.4 <sup>b</sup>
	10	17.8 ± 3.2 <sup>b</sup>
	20	19.5 ± 0.4 <sup>b</sup>

Antibacterial activity was expressed as average ± standard deviation. Culture media (g/l): 1 [yeast extract, 3; soluble starch 5; NH<sub>4</sub>(SO<sub>4</sub>)<sub>2</sub>, 2]; 2 [malt extract, 10; yeast extract, 4; dextrose, 4], 3 [soluble starch, 10; yeast extract, 4; peptone, 2; CaCO<sub>3</sub>, 10; Fe (SO<sub>4</sub>)<sub>3</sub>, 8], and 4 [dextrose, 32.5; soy trypticase broth, 9]. –, not activity. Different letters mean significant differences among the conditions of each parameter, for a 95% level of confidence (multiple range test)

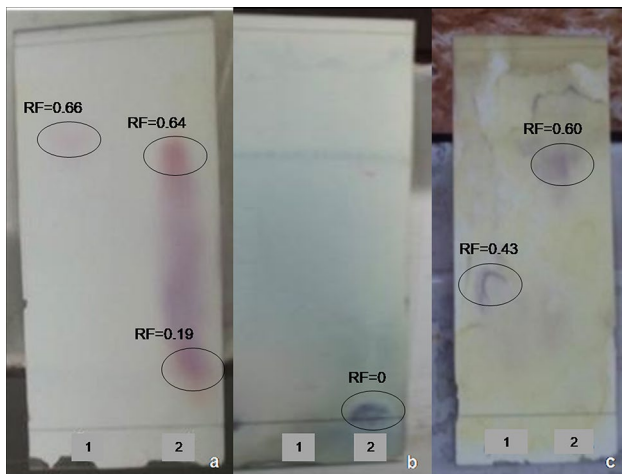


**Fig. 4** Chemical characterization of the BMs produced by *B. velezensis* A3. **(a)** TLC plate sprayed with ninhydrin solution (0.2% in distilled water) produced blue violet spots indicating the presence of peptides/amino acids **(b)** TLC plate sprayed with 10% (v/v) fosfomolibdic acid in absolute ethanol produced blue spots indicating the presence of lipids, and **(c)** TLC plate sprayed with MTT showing the presence of reducing sugars (violet spots) in the (1) petroleum and (2) n-butanol extracts

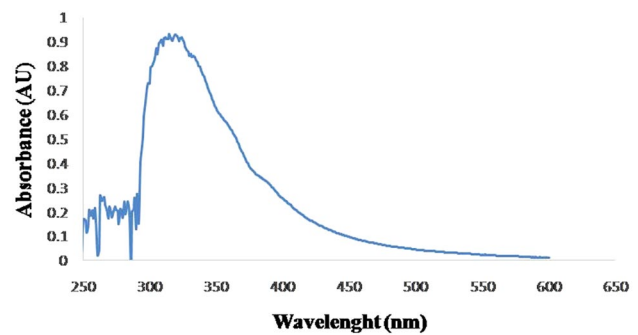


**Fig. 5** UV-Vis spectra of the cell-free supernatant of *B. velezensis* A3 at wavelengths of 250–600 nm

useful compounds, which may serve not only as direct drugs but also as lead compounds for structural modifications and templates for the rational drug design [28]. Here, a strain named A3 isolated during the course of bioprospecting study from a freshwater sediment was chosen by its antibacterial and antifungal potentials for its taxonomic identification and characterization of its (their) bioactive metabolite(s).

Classification and identification of antibiotic-producing species are utmost importance in the dereplication process of natural products. MALDI-TOF MS is one of the high-throughput techniques that has emerged in the last years for rapid identification and dereplication microbial [29]. In this study, the isolate A3 had an incongruent identification when the main mass profile was obtained toward two close-related species from *Bacillus subtilis* strains complex: *B. amyloliquefaciens* and *B. methylotrophicus*. Close relatedness of species has been documented as a challenge for MALDI-TOF MS identification at species level [10, 30]. On the other hand, 16S rRNA gene has been used in the typing of numerous bacteria and for constructing bacterial phylogenetic relationships. However, our results and previous studies demonstrated that this gene is not sufficiently divergent to delimit the phylogeny of *Bacillus subtilis* species complex [11]. Many authors consider that the evolution rate of protein-encoding genes is higher than 16 rRNA gene, being an alternative to delimit close-related species [12]. At last, the analysis of the *gyrA* gene sequence allowed grouping of strain A3 in the monophyletic clade of *B. amyloliquefaciens* subsp. *plantarum* strains (Fig. 2), now reclassified as a heterotypic synonym of *B. velezensis* [31], which corroborates the value of this gene as discriminative phylogenetic marker within the *B. subtilis* group [26].

*B. velezensis* A3 showed antibacterial and antifungal properties. These activities could be related with amphiphilic molecules such as lipopeptides which have marked antimicrobial activity against pathogens [32–34]. Biocontrol



effects against Gram-positive bacteria similar to those reported in this study have been referred by other researchers for this species. In concordance with our results, Baharudin et al. [35] demonstrated the activity of *B. velezensis* against methicillin-resistant *S. aureus* strains, but with lower activity than the determined in our study against *S. aureus* ATCC 700699. The activity revealed for *B. velezensis* A3 against MRSA strains becomes relevant, since this coccus has developed multiple resistance mechanisms against antibiotics, being a serious problem for the worldwide public health. This antibacterial activity of *B. velezensis* A3 could be due to surfactins which are lipopeptides with a recognized antibacterial activity. They have been found to be active against multidrug-resistant bacteria, either disrupting the bacterial cell membrane via pore formation with a subsequently cell lysis or entering the cell; and/or inhibiting essential intracellular functions by binding to nucleic acids or intracellular proteins [36, 37]. In addition, it is well known that *B. velezensis* is able to produce other potent antibacterial agents that include bacillaene, bacilysin, bacillomycin-D, bacillibactin, diffidicin, and macrolactin [34].

The cell-free supernatant of *B. velezensis* A3 inhibited the radial growth of the tested phytopathogens. The PIGR (53%) of *A. alternata* CECT 2662 was higher to that reported by Silva et al. [38]. In a study, Meena et al. [39] showed that surfactins and iturins from lipopeptide fraction of *B. velezensis* KLP201 inhibited the growth of *A. niger* by  $45.0 \pm 1.2\%$ . In this study, the results showed an inhibition of 35%. Therefore, pure compounds of the active fraction of the extract of the strain A3 might exceed the previously reported value. Our results also demonstrated that the bioactive compounds of *B. velezensis* produced alterations in the structure and morphology of the hyphae (Fig. 3), which were comparable with those obtained by Orberá et al. [40] when tested the strain *Bacillus subtilis* SR/B-16 against phytopathogenic fungi. Iturins and fengycins, the best characterized bioactive lipopeptides of *Bacillus* with antifungal activity, limit normal mycelium growth due to their ability to perturb fungal cell membrane integrity resulting in cytoplasm leakage and finally hyphae death [34, 41]. These compounds can also act in the inhibition of spore germination. Surfactins are also mentioned as antifungal compounds by inhibiting the glucan synthase involve in cell wall synthesis of fungi and inducing apoptotic markers [32, 42].

Preliminary characterization of the BMs produced by *Bacillus velezensis* A3 revealed the presence of both lipid and peptide compounds. Although these compounds could be part of either culture medium or remain of cellular structural components, Rf-values are in concordance with those reported for lipopeptides compounds in previous studies [32, 34, 39]. The presence of these compounds was also corroborated using a UV-Visible spectroscopy. Usually, peptides/amino acids absorb ultraviolet light at

wavelength of 260–280 nm. Nonetheless, its maximum wavelength and intensity of the absorption bands depend of the amino acid backbone. Characteristic bands of amino acids with aromatic residues could be the responsible of the nascent band at 293 nm. On the other hand, the spectrum revealed the presence of vibrational components of transitions  $\pi-\pi^*$  due to unsaturations by multiple bonds. An increase in conjugation causes the band to be bathochromically shifted to longer wavelengths. Molecules with four or more conjugated double bonds associated with some chromophores, which correspond to lipids, have their maximum at values of 300 nm or more. The results of this study suggest either the presence of aromatic structures of the related amino acids or the presence of lipids with four or more conjugated unsaturations, giving as result a bathochromic shift at a maximum of 315 nm. Meena et al. [43] showed peaks with maximum between 201 and 382 nm for the pure lipopeptides iturin A and surfactin. Qiu and Kirsh [44] obtained a wide band around 330–380 nm in a UV spectrum of the daptomycin, an antistaphylococcal lipopeptide produced by *Streptomyces roseosporus*. The presence of tryptophan in this molecule makes a bathochromic shift toward these wavelengths.

The presence of both peptides/amino acids and lipids compounds in the culture of *B. velezensis* A3 allowed us to hypothesize about the lipopeptide nature of the bioactive compounds produced by the strain A3, such as have been already mentioned in previous reports for this species [32, 34, 39]. Lipopeptides are amphiphilic molecules that contain a lipophilic fatty acid chain and a hydrophilic peptide ring. Still, an extraction and purification process of the compounds, and a deep characterization by high-performance chromatography and spectroscopic methods should be performed to know the real nature of the BMs related with the antibacterial and antifungal activities of *B. velezensis* A3.

The influence of culture conditions on lipopeptide production was previously described for other strains of *Bacillus* [45–47]. *B. velezensis* A3 was able to grow in the media 1 and 3 but did not produce BMs. Starch has been described by enhancing the microbial metabolism [48], but the degradation of this complex carbon source by A3 for metabolite production and lack of glucose in these culture media could be the reasons of this result. A high concentration of glucose triggers the metabolite repression and production of undesirable metabolites [47, 48]. However, most studies have shown that glucose concentration at 20–40 g/l favors lipopeptide production [45, 47]. Antimicrobial activity using the media 2 and 4, with glucose at 4 and 32.5 g/l, respectively, supports the above mentioned (Table 1). ISP2 (medium 2) has been the most suitable to produce BMs by Actinobacteria. It contains low amount of glucose and readily available nitrogen sources (malt extract and yeast extract).

Differences in composition likely account for the antibacterial results, such as showed the media 2 ( $8.25 \pm 0.4$  mm) and 4 ( $7.0 \pm 0.00$  mm).

Maximum BMs production by *B. velezensis* A3 was yielded at the 96 h, which is in concordance with other studies [47, 49, 50]. It is well known that bioactive metabolites are produced either at the end of log phase or in the stationary phase of growth when nutrients become depleted [51]. Our results evidenced no significant differences in the BMs production when the medium is adjusted at pH 8–9, with a maximum at pH 8. Similar results were obtained by Jamil et al. [49] in the antibiotic production by *B. subtilis* MH-4. Nor the inoculum size (5, 10, and 20%) had effect in the production of BMs by *B. velezensis* A3. Nonetheless, it has great influence in the duration of lag phase, specific growth rate, biomass yield, and quantity of the final product [50].

## Conclusions

In this study, we isolated and identified a *Bacillus* sp. with antibacterial and antifungal activity: *Bacillus velezensis* A3. The preliminary characterization of A3's bioactive compounds evidenced the presence of lipids and peptides in the culture, which might suggest the lipopeptide nature thereof. The lipopeptides are a novel class of potent versatile weapons by this bacterium to deal with a variety of pathogens. *Bacillus velezensis* A3 could be considered as a potential alternative to treat pathogens in the biopharmaceutical industry and agriculture.

**Supplementary Information** The online version contains supplementary material available at <https://doi.org/10.1007/s00284-022-03090-2>.

**Acknowledgements** The authors would like to thanks to the BCCM/LMG Bacterial Collection regarding bacterial identification. We appreciate the help of Prof. dr. Paul Cos (Department of Pharmaceutical Sciences, University of Antwerp, Belgium), and Eliza Depoorter (Laboratory of Microbiology, Faculty of Sciences, Ghent University, Belgium) for the help with antibacterial activity by broth microdilution and overlay methods, respectively.

**Author Contributions** MIC Conceptualization, Performing experiments, Analysis, and Interpretation of data, Writing—Original Draft; SR & GLL Conceptualization, Writing—Review & Editing; PV Resources, Critical revision of the article; AW Resources, Analysis, and interpretation of data; AF Analysis and Interpretation of data; JG, DR, JB, YL, LP, & TLM Performing experiments. All authors read and approved the final manuscript.

**Funding** This work was supported by the VLIR-UOS (Flemish Inter-university Council-University Cooperation for Development) in the context of the Institutional University Cooperation Program with Universidad de Oriente; especially, by means of the P-3 project “Natural Products and Pharmaceutical Services to improve the patient quality of life in Eastern Cuban Hospital's,” The BCCM/LMG Bacteria Collection is supported by the Federal Public Planning Service—Science Policy, Belgium.

**Data Availability** All data generated during this study are included in this article and its supplementary information file.

**Code Availability** Not applicable.

## Declarations

**Conflict of interest** The authors declare that there are no conflicts of interest.

**Ethical Approval** This article does not contain any studies with human participants or animals.

**Consent for Publication** Not applicable.

**Consent to Participate** Not applicable.

## References

- Zhi-Wen Y, Yan-Li Z, Man Y, Wei-Jun F (2015) Clinical treatment of pandrug-resistant bacterial infection consulted by clinical pharmacist. *Saudi Pharm J* 23:377–380
- Mann A, Nehra K, Rana JS, Dahiya T (2021) Antibiotic resistance in agriculture: perspectives on uncoming strategies to overcome upsurge in resistance. *Sciences* 2:10030
- Viswanathan VK (2014) Off-label abuse of antibiotics by bacteria. *Gut Microbes* 5:3–4
- Shafi J, Tian H, Ji M (2017) *Bacillus* species as versatile weapons for plant pathogens: a review. *Biotechnol Biotech Equip* 31:446–459
- Eon JS, Choi HS (2016) Inhibition of *Bacillus cereus* growth and toxin production by *Bacillus amyloliquefaciens* RD7-7 in fermented soybean products. *J Microbiol Biotechnol* 26:44–55
- Lee JY, Shim JM, Yao Z, Liu X, Lee KW, Kim HJ, Ham KS, Kim JH (2016) Antimicrobial activity of *Bacillus amyloliquefaciens* EMD17 isolated from *Cheonggukjang* and potential use as a starter for fermented soy foods. *Food Sci Biotechnol* 30(25):525–532
- Singhal N, Kumar M, Kanaujia PK, Viridi JS (2015) MALDI-TOF mass spectrometry: an emerging technology for microbial identification and diagnosis. *Front Microbiol* 6:791
- AlMasoud N, Xu Y, Nicolaou N, Goodacre R (2014) optimization of matrix assisted laser desorption/ionization time of flight mass spectrometry (MALDI-TOF-MS) for the characterization of *Bacillus* and *Brevibacillus* species. *Anal Chim Acta* 840:49–57
- Ha M, Jo HJ, Choi EK, Kim Y, Kim J, Cho HJ (2019) Reliable identification of *Bacillus cereus* group species using low mass biomarkers by MALDI-TOF MS. *J Microbiol Biotechnol* 29:887–896
- Cuénod A, Foucault F, Pflüger V, Egli A (2021) Factors associated with MALDI-TOF mass spectral quality of species identification in clinical routine diagnostics. *Front Cell Infect Microbiol* 11:646648
- Rooney AP, Price NP, Ehrhardt C, Swezey JL, Bannan JD (2009) Phylogeny and molecular taxonomy of the *Bacillus subtilis* species complex and description of *Bacillus subtilis* subsp. *inaquosorum* subsp. nov. *Int J Syst Evol Microbiol* 59:2420–2436
- Vandamme P (2007) Taxonomy and classification of bacteria. In: Murray PR, Baron EJ, Jorgenson JH, Landry ML, Pfaller MA (eds) *Manual of clinical microbiology*, 9th edn. DC, USA, Washington, pp 275–290

13. Bauer AW, Kirby WMM, Sherris JC, Turck M (1966) Antibiotic susceptibility testing by a standardized single disk method. *Am J Clin Pathol* 36:493–496 (PMID: 5325707)
14. Tagg JR, McGiven AR (1971) Assay system for bacteriocins. *Appl Microbiol* 21:943–943
15. Méndez D, Escalona-Arranz J, Foubert K, Matheeußen A, Van der Auwera A, Piazza S, Cuyper A, Cos P, Pieters L (2021) Chemical and pharmacological potential of *Coccoloba cowellii*, an endemic endangered plant from Cuba. *Molecules* 26(4):935
16. Wieme AD, Spitaels F, Aerts M, De Bruyne K, Landschoot AV, Vandamme P (2014) Effects of growth medium on matrix-assisted laser desorption-ionization time of flight mass spectra: a case study of acetic acid bacteria. *Appl Environ Microbiol* 80:1528–1538
17. Niedermeyer THJ, Strohm M (2012) mMass as a software tool for the annotation of cyclic peptide tandem mass spectra. *PLoS ONE* 7:e44913
18. Snauwaert I, Papalexandratou Z, De Vuyst L, Vandamme P (2013) Characterization of strains of *Weissella fabalis* sp. nov. and *Fructobacillus tropaeoli* from spontaneous cocoa bean fermentations. *Int J Syst Evol Microbiol* 63:1709–1716
19. Yoon SH, Ha SM, Kwon S, Lim J, Kim Y, Seo H, Chun J (2017) Introducing EzBioCloud: a taxonomically united database of 16S rRNA and whole genome assemblies. *Int J Syst Evol Microbiol* 67:1613–1617
20. Pruesse E, Peplies J, Glöckner FO (2012) SINA: accurate high-throughput multiple sequence alignment of ribosomal RNA genes. *Bioinform* 28:1823–1829
21. Saitou N, Nei M (1987) The neighbor-joining method: a new method for reconstructing phylogenetic trees. *Mol Biol Evol* 4:406–425
22. Felsenstein J (1981) Evolutionary trees from DNA sequences: a maximum likelihood approach. *J Mol Evol* 17:368–376
23. Fitch WM (1971) Toward defining the course of evolution: minimum change for a specific tree topology. *Syst Zool* 20:406–416
24. Kumar S, Stecher G, Tamura K (2016) MEGA7: molecular evolutionary genetics analysis version 7.0 for bigger datasets. *Mol Biol Evol* 33:1870–1874
25. Kimura M (1980) A simple method for estimating evolutionary rate of base substitutions through comparative studies of nucleotide sequences. *J Mol Evol* 16:111–120
26. Chun J, Bae KS (2000) Phylogenetic analysis of *Bacillus subtilis* and related taxa based on partial *gyrA* gene sequences. *Antonie Van Leeuwenhoek* 78:123–127
27. Edgar RC (2004) MUSCLE: multiple sequence alignment with high accuracy and high throughput. *Nucleic Acids Res* 32:1792–1797
28. Bérty J (2005) Bioactive microbial metabolites: a personal view. *J Antibiot* 58:1–26
29. Huschek D, Witzei K (2019) Rapid dereplication of microbial isolates using matrix-assisted laser desorption ionization time-of-flight mass spectrometry: a mini-review. *J Adv Res* 19:99–104
30. Han SS, Jeong YS, Choi SK (2021) Current scenario and challenges in the direct identification of microorganisms using MALDI TOF MS. *Microorganisms* 9:1917
31. Dunlap C, Kim SJ, Kwon SW, Rooney A (2016) *Bacillus velezensis* is not a later heterotypic synonym of *Bacillus amyloliquefaciens*, *Bacillus methylotrophicus*, *Bacillus amyloliquefaciens* subsp. *plantarum* and '*Bacillus oryzicola*' are later heterotypic synonyms of *Bacillus velezensis* based on phylogenomics. *Int J Syst Evol Microbiol* 66:1212–1217
32. Toral L, Rodríguez M, Béjar V, Sampedro I (2018) Antifungal activity of lipopeptides from *Bacillus* XT1 CECT 8661 against *Botrytis cinerea*. *Front Microbiol* 9:1315
33. Li X, Gao X, Zhang S, Jiang Z, Yang H, Liu X, Jiang Q, Zhang X (2020) Characterization of a *Bacillus velezensis* with antibacterial activity and inhibitory effect on common aquatic pathogens. *Aquac* 523:735165
34. Rabbee MF, Baek KH (2020) Antimicrobial activities of lipopeptides and polyketides of *Bacillus velezensis* for agricultural applications. *Molecules* 25(21):4973
35. Baharudin M, Ngalimat MS, Mohd Shariff F, Balia Yusof ZN, Karim M, Baharum SN, Sabri S (2021) Antimicrobial activities of *Bacillus velezensis* strains isolated from stingless bee products against methicillin-resistant *Staphylococcus aureus*. *PLoS ONE* 16:e0251514
36. Pokhrel R, Bhattarai N, Baral P, Gerstman BS, Park JH, Handfield M, Chapagain PP (2019) Molecular mechanisms of pore formation and membrane disruption by the antimicrobial lantibiotic peptide Mutacin 1140. *Phys Chem Chem Phys* 21(23):12530–12539
37. Benfield AH, Henriques ST (2020) Mode-of-action of antimicrobial peptides: membrane disruption vs intracellular mechanisms. *Front Med Technol*. <https://doi.org/10.3389/fmedt.2020.610997>
38. Silva M, Pereira A, Teixeira D, Candeias A, Caldeira AT (2016) Combined use of NMR, LC-ESI-MS and antifungal tests for rapid detection of bioactive lipopeptides produced by *Bacillus*. *Adv Microbiol* 6:788–796
39. Meena KR, Tandon T, Sharma A, Kanwar SS (2018) Lipopeptide antibiotic production by *Bacillus velezensis* KLP2016. *J App Pharm Sci* 8(03):091–098
40. Orberá TM, Serrat MJ, Ortega E (2014) Potential applications of *Bacillus subtilis* strain SR/B-16 for the control of phytopathogenic fungi in economically relevant crops. *Biotechnol Appl* 31:7–12
41. Andrić S, Meyer T, Ongena M (2020) *Bacillus* responses to plant-associated fungal and bacterial communities. *Front Microbiol* 11:1350
42. Grady EN, MacDonald J, Ho MT, Weselowski B, McDowell T, Solomon O, Renaud J (2019) Yuan ZC (2019) Characterization and complete genome analysis of the surfactin-producing, plant-protecting bacterium *Bacillus velezensis* 9D-6. *BMC Microbiol* 19:5
43. Meena KR, Sharma A, Kumar R, Kanwar SS (2020) Two factor at a time approach by response surface methodology to aggrandise the *Bacillus subtilis* KLP2015 surfactin lipopeptide to use as antifungal agent. *J King Saud Univ Sci* 32:337–348
44. Qiu J, Kirsh LE (2014) Evaluation of lipopeptide (Daptomycin) aggregation using fluorescence, light scattering, and nuclear magnetic resonance spectroscopy. *J Pharm Sci* 103(3):853–861
45. Hmidet N, Aayed HB, Jacques P, Nasri M (2017) Enhancement of surfactin and fengycin production by *Bacillus mojavensis* A21: application for diesel biodegradation. *BioMed Res Int* 3:1–8
46. Phulpoto IA, Yu Z, Hu B, Wang Y, Ndayisenga F, Li J, Liang H, Qazi MA (2020) Production and characterization of surfactin-like biosurfactant produced by novel strain *Bacillus nealsonii* S2MT and its potential for oil contaminated soil remediation. *Microb Cell Fact* 19:145
47. Barale SS, Ghane SG, Sonawane KD (2022) Purification and characterization of antibacterial surfactin isoforms produced by *Bacillus velezensis* SK. *AMB Express* 12(1):7
48. Pournajati R, Karbalaee-Heidari HR (2020) Optimization of fermentation conditions to enhance cytotoxic metabolites production by *Bacillus velezensis* strain RP137 from the Persian Gulf. *Avicenna J Med Biotechnol* 12(2):116–123
49. Jamil B, Hasan F, Hameed A, Ahmed S (2007) Isolation of *Bacillus subtilis* MH-4 from soil and its potential of polypeptidic antibiotic production. *Pak J Pharm Sci* 20(1):26–31
50. Ghribi D, Ellouze-Chaabouni S (2011) Enhancement of *Bacillus subtilis* lipopeptide biosurfactants production through optimization of medium composition and adequate control of aeration. *Biotech Res Int* 2011:1–6
51. Nehal N, Singh P (2021) Optimization of cultural condition of *Bacillus* sp. MZ540316: improve biodegradation efficiency of

lipopeptide biosurfactant against polyethylene. *Biomass Conv Bioref.* <https://doi.org/10.1007/s13399-021-02042-3>

**Publisher's Note** Springer Nature remains neutral with regard to jurisdictional claims in published maps and institutional affiliations.

Springer Nature or its licensor (e.g. a society or other partner) holds exclusive rights to this article under a publishing agreement with the author(s) or other rightsholder(s); author self-archiving of the accepted manuscript version of this article is solely governed by the terms of such publishing agreement and applicable law.